

# Overcoming Low- $I_Q$ Challenges in Low-Power Applications

---



## **Keith Kunz**

Distinguished Member Technical Staff  
Design Engineer & Technologist, Linear Power

## **Stefan Reithmaier**

Distinguished Member Technical Staff  
Analog Design Manager, Boost & Multi Channel/Phase DCDC

**TI POWER**

# Designers of ultra-low-power electronics today make constant trade-offs between higher performance and longer battery life. Despite improved battery capacities, the fundamental challenge remains: How do we achieve higher performance for longer periods of time?

## At a glance

This paper examines the need for and associated challenges and solutions to reduce quiescent current ( $I_Q$ ).



### 1 What is $I_Q$ ?

$I_Q$  is the no-load quiescent current, and the most important bottleneck to overcome for duty-cycled low-power systems. Low  $I_Q$  enables longer battery life.



### 2 Why low $I_Q$ creates new challenges

Reducing  $I_Q$  creates trade-offs in transient noise performance, die package area and output power range.



### 3 How to break low- $I_Q$ Barriers

Reducing  $I_Q$  by decades without sacrificing performance or area requires a reexamination of both silicon technologies and circuit techniques.

Minimizing quiescent current ( $I_Q$ ) is a key factor to reduce power consumption and manage battery life. An Internet-of-Things (IoT) sensor node is one of the best examples of why it's important to minimize  $I_Q$  to extend battery life. For example, in the low-power IoT application shown in [Figure 1](#), the SimpleLink™ MCU controls a door lock via Bluetooth®, a Wi-Fi® connection or both.

Because these types of systems spend the majority (>99%) of the time in standby mode, as shown in [Figure 2](#), the  $I_Q$  in standby or sleep mode tends to be the limiting factor for battery life. Careful optimization of low- $I_Q$  power-management blocks makes it possible to extend battery life from two years to more than five years.

Standby  $I_Q$  has long been a concern, but historically solutions were limited to a narrow set of low-power systems. Recent breakthroughs reduced the  $I_Q$  in power-management building blocks like DC/DC converters, power switches, low-dropout regulators (LDOs) and supervisors, widening the use of these blocks to end equipment such as industrial meter applications, automotive sensors and personal wearables.

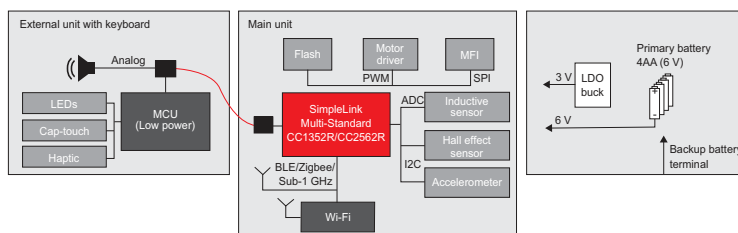


**Figure 1.** Smart e-lock block diagram.

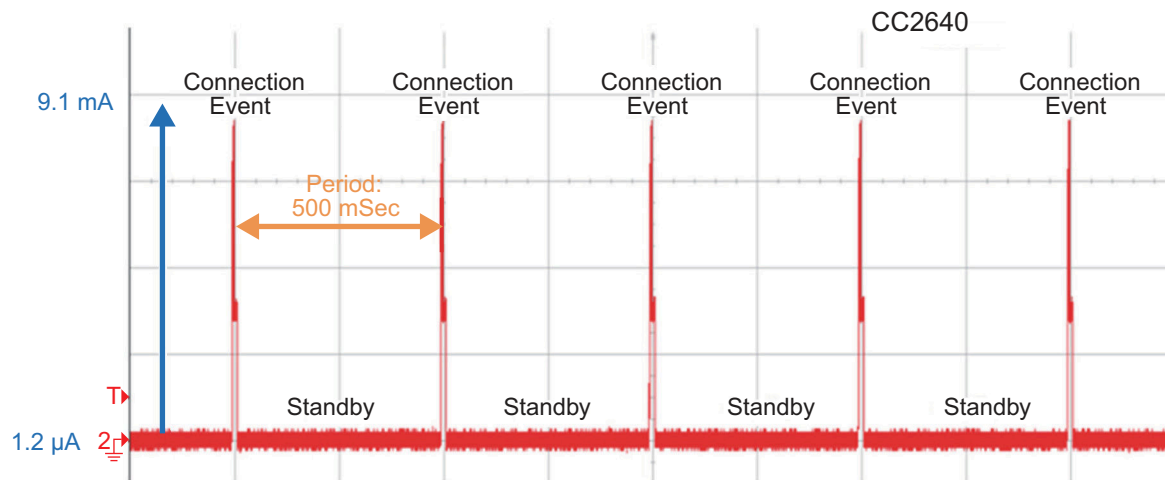


**Figure 2.** Current consumption vs. time in a smart e-lock.

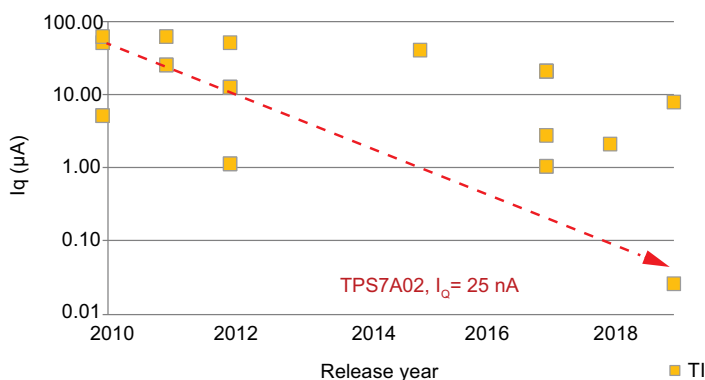


**Figure 3.** 5-V LDO  $I_Q$  over time.

As [Figure 3](#) illustrates, the  $I_Q$  in 5-V LDOs has approximately reduced 90% every three years over the past 10 years. Both circuit improvements and optimized process technologies have enabled the reduction of solution area and improved transient-noise performance, while simultaneously reducing  $I_Q$ .

## Contributors to $I_Q$

$I_Q$  is the amount of current used when the integrated circuit (IC) is enabled but not switching nor supporting an external load current. Shutdown current ( $I_{SHDN}$ ) is the current drawn from the supply when the device is disabled.

The  $I_Q$  of always-on functions such as power regulators contribute to the overall  $I_Q$  of systems with long standby times. Inside the power regulators themselves, the voltage reference, error amplifier, output voltage divider

and protection circuits all have their own operating currents.

To determine the total  $I_Q$  drawn from a battery or power supply, you must consider the always-on functions and leakage sources from capacitors, resistors and inductors.

For the  $I_Q$  of switching converters, we must make some distinctions. Switching converters usually include a power-save mode that enables a longer non-switching period, thereby reducing average  $I_Q$ . But because the  $I_Q$  does not include switching currents or the efficiency component of currents drawn from the voltage output ( $V_{OUT}$ ), like in the example of a boost converter in [Figure 4](#), we can use [Equation 1](#) to calculate a superset of the input-referred no-load operating currents for almost any regulator as:

$$I_{I(standby)} = I_Q(V_{in}) + I_{Leakage}(V_{in}) + \frac{V_{out}}{V_{in} \times \eta \Gamma} \times [I_Q(V_{OUT}) + I_{FB} + I_{LOAD}] \quad (1)$$

Currents and voltages are explained in [Figure 4](#), where:

- $I_Q(V_{IN})$  is the  $V_{IN}$ -referred  $I_Q$  (the IC data-sheet value).
- $I_{Leakage}(V_{IN})$  is the leakage drawn on the  $V_{IN}$  pin from capacitors, inductors, diodes or switches.
- $V_{OUT}$  is the output voltage.
- $V_{IN}$  is the battery voltage (the input voltage to the LDO, boost or buck-boost converter).

- $\eta_1$  is the DC/DC efficiency when the converter is switching.
- $I_Q(V_{OUT})$  is the  $I_Q$  drawn on the switching converter's  $V_{OUT}$  pin. For an LDO,  $I_Q(V_{OUT}) = 0$ .
- $I_{FB}$  is the current of the feedback resistor divider, if applicable.
- $I_{Load}$  is the load current potentially present on  $V_{OUT}$  in standby mode.

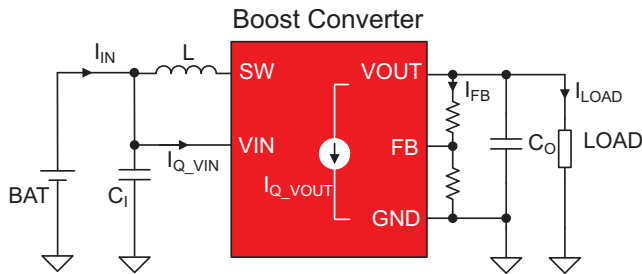


**Figure 4.** Currents in a boost converter system.

If you know the battery capacity and have calculated the input-referred standby current, **Equation 2** estimates the battery life for a heavily duty-cycled low-power system in standby mode >99.9% of the time as:

$$\text{Battery Lifetime} = \frac{\text{Battery Capacity}}{I_{I(\text{standby})} + I_{\text{Battery leakage}}} \quad (2)$$

For example, the battery of a duty-cycled system with 1.2  $\mu\text{A}$  of standby current can last as 8.7 years on a 100-mAh coin-cell battery.

## Why low $I_Q$ creates new challenges

Let's look at some of the reasons why it's so challenging to reduce  $I_Q$ .

### Transient response

Power-supply accuracy is often limited by its transient response, which is characterized by its maximum voltage drop, settling time and voltage error integral (**Figure 5**).

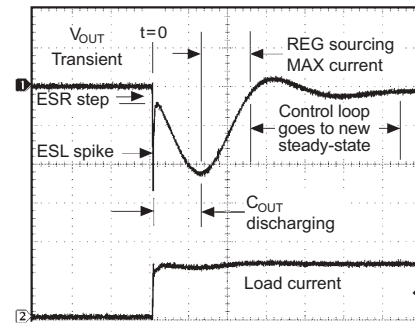


**Figure 5.** An output voltage transient.

The response time measures how fast a power device regulates back to the targeted output voltage after an abrupt change in load current or supply voltage. The response time comprises three stages: a delay time to react to the change, a recovery time from a dip or overshoot, and a settling time.

Low- $I_Q$  devices suffer from longer response times because the internal parasitic capacitors need to be charged to new operating points with relatively less current. The worst case is usually a step from no load to the maximum allowed load current. Such cases necessitate reactivating circuits that had been deactivated or reduced in power, causing an additional delay.

More importantly, the settling time itself suffers from reduced bias conditions. For a conventional differential input stage, the gain reduces linearly with the bias current, which causes a reduction in bandwidth and increased settling time.

Calculating figures of merit (FOMs) helps the designer judge the overall performance of a power regulator.

**Equation 3** calculates a transient response dip FOM, normalizing the  $I_Q$  by the maximum output current of the converter, the load current step ( $\Delta I_O$ ), the induced voltage drop ( $\Delta V_O$ ) and the output capacitor ( $C_O$ ). **Figure 6** shows how FOM changes over time for a 5-V buck-boost converter. The smaller the FOM, the better the regulator's performance.

$$\text{transient response dip FOM} = \frac{I_Q \cdot \Delta V \cdot C_O}{I_{O\_MAX} \cdot \Delta I_O} \quad (3)$$

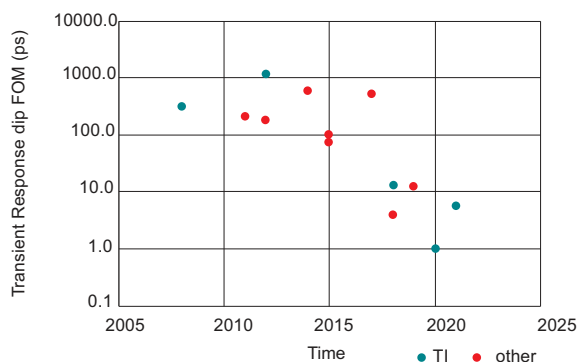


**Figure 6.** Transient response dip FOM over time for a 5-V buck-boost converter.

## Ripple

Another way to enable lower  $I_Q$  is to enter different power-save modes depending on the load current. While the transition between these modes is usually automatic, the implementation and performance differ significantly. Two points of concern are the voltage ripple during the transition between power-save modes and the output-voltage accuracy. Because operating conditions (such as in an error amplifier) are usually different in each power-save mode, the transition time required to adjust to the different operating points can directly result in errors on the output voltage. Additionally, comparator delays will be longer at lower biasing currents, potentially causing inaccuracies for both the voltage threshold and zero-current detection, which could result in higher output-voltage ripple.

## Noise

Another hurdle to overcome is the increased self-noise in amplifiers that accompany lower  $I_Q$  biasing. The internal blocks seen in **Figure 7** contributing the most noise in LDOs are the reference system (band gap), error amplifier and resistor-divider that scales the output voltage.

**Figure 8** shows a typical noise profile vs frequency. The two main types of noise generated from these blocks are:

- Thermal noise (also called  $4kTR$  noise) is a particular concern for ultra-low- $I_Q$  designs because it is linearly proportional to the resistance used. Both resistor-derived bias currents used in the error amplifier and reference blocks, and the resistance used in resistor

dividers, are dominant contributors to thermal noise at frequencies  $>1$  kHz.

- Flicker noise (also called  $1/f$  noise) is a low-frequency noise  $<100$  Hz, that can be mitigated by increasing the sizes of differential pairs in the reference system and error amplifiers. This larger sizing however creates obstacles for nano-power designs, as they increase self-induced leakage and add more capacitance, which slows down response times.

A simple method to evaluate the resultant noise for a given  $I_Q$  is to multiply the integrated noise over the frequency range of concern and the  $I_Q$  at the operating point of interest. You can usually find both numbers on device data sheets.

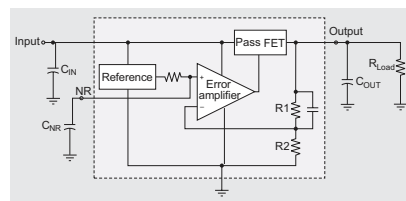


**Figure 7.** Simplified LDO block diagram.

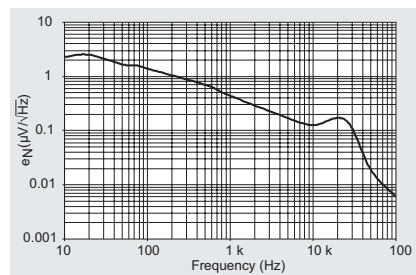


**Figure 8.** Spectral noise density example.

## Die size and solution area

Decreased  $I_Q$  may also result in increased board area required for larger passives or IC package sizes. Larger external passives such as large-value capacitors for both LDOs and DC/DC converters are common in nanopower devices and typically used to compensate for poorer transient performance. Larger package areas are directly attributable to larger die areas.

Upon visual inspection of die teardowns with an  $I_Q < 1 \mu A$ , resistors and capacitors make up more than

20% of the internal non-field-effect-transistor (FET) die area. While there are multiple solutions to solve  $I_Q$ -area problems, an easy method to filter out the best solutions on the market is to apply a simple FOM:  $I_Q$  multiplied by the smallest package area. You can access the FOM by pulling relevant information from data sheets; looking at the smallest package offered provides clues about smaller die areas.

Choosing the device with both the lowest  $I_Q$  and smallest package available usually means good  $I_Q$ -area efficiency.

### Leakage and subthreshold operation

The goals of a nanopower process can conflict with the goals of high-performance deep-submicron technologies, which prioritize speed and gate density over  $I_Q$  reduction. While process technologies may vary, the vast majority of leakages come from large digital circuits, memory and high-power FETs. The accuracy of always-on circuitry tends to be limited to the controllability of components like resistors and capacitors and a mismatch between transistors. Not having the right components to address the leakage and control of always-on circuits manifests itself in large typical and worst-case  $I_Q$  and  $I_{SHDN}$  ratios across temperature. A dedicated low-power process technology with the right components can provide a clear manufacturing advantage.

One fundamental challenge is to reliably operate components biased in the subthreshold region. One

common problem seen is increased random threshold voltage ( $V_T$ ) mismatch. **Figure 9** shows a mechanism reported in literature that increases random mismatch by a thinning of oxide in the shallow trench isolation (STI) at the edge of the transistor. This parallel low- $V_T$  edge transistor seen in **Figure 9**, distorts the  $V_T$  of the intentional transistor, resulting in much higher random mismatch for the most basic analog circuits like differential pairs and current mirrors. These mismatches can degrade the output voltage or mode control accuracy over temperature which can be clearly observed in the data sheet.

### How to break low $I_Q$ barriers

Optimizing  $I_Q$  requires the resolution of multiple, conflicting design challenges. You must meet all of the critical performance specifications in transient response, noise and accuracy, while reducing  $I_Q$  by orders of magnitude. Before assessing the trade-offs in performance specifications, you must quantify the  $I_Q$  and power losses over the entire output load range. For DC/DC switching converters, look at the power efficiency over load current, while for LDOs, look at current efficiency over load current.

As an example, **Figure 10** shows the efficiency of TI's **TPS63900** buck-boost converter versus competition. The efficiency for TPS63900 stays above 80% over six decades of load current, starting at 1  $\mu A$  and hitting a peak efficiency of 96%.

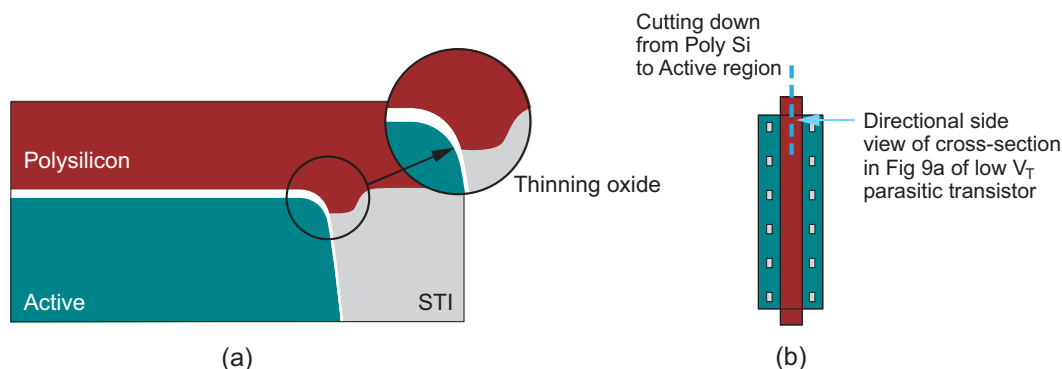


**Figure 9.** Oxide-thinning-induced parasitic low- $V_T$  in 2D cross-section (a); and layout view (b).



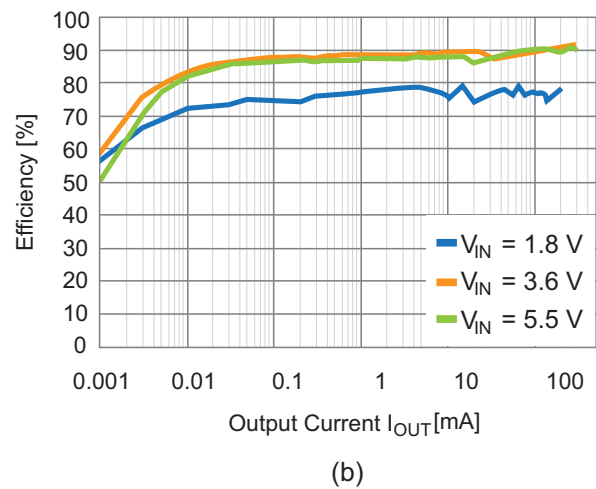
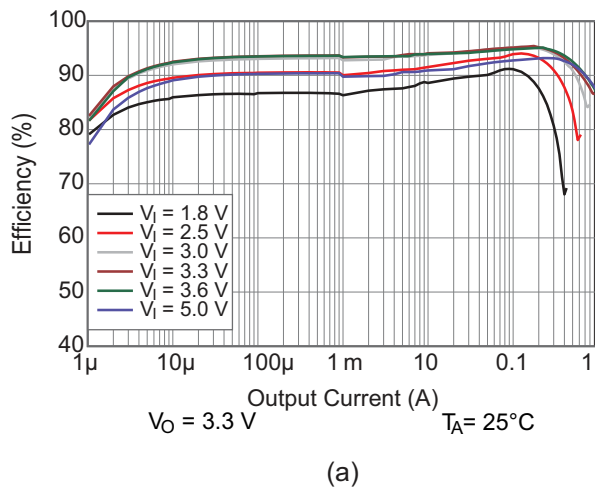


**Figure 10.** Efficiency of the TPS63900 (a) and competition (b). (Source: TI and competitor data sheets).

### Addressing transient response issues

The key to improving the transient response is to start with the best topology. For example, the TPS61094 supports low  $I_Q$  and fast transient response. The TPS61094 is a bi-directional buck/boost converter that has a low  $I_Q$  of 60 nA in supercapacitor-charging (buck) and supercapacitor-discharging (boost) modes. The TPS61094 monitors  $dv/dt$  slopes at the output and adjusts its regulation behavior to optimize the transient performance at any given moment. This allows to quickly detect an output voltage drop while maintaining low  $I_Q$  at the same time. As a result, the output voltage will remain nearly constant when the TPS61094 starts supporting backup power or peak load support from a supercapacitor.

You must reduce the number of current-consuming blocks as much as possible, so the simpler the topology, the better. For example, the TPS63900 four-switch buck-boost converter, which has an  $I_Q$  of 75 nA, uses one single mode to regulate the output voltage above, below or equal to the input level. Besides the core architecture, using sample-and-hold techniques when entering light load minimizes the  $I_{SHDN}$  of all internal support functions.

You can conserve even more current with a zero-current feedback divider, digital assisted control and dynamic

biasing. Dynamic biasing is a well-known technique, but becomes challenging when operating with just a few nanoamperes. To avoid the gain falloff at low bias currents, optimally shaping both the transconductance and output resistance as a function of the bias current achieves an  $I_Q$ -efficient constant gain amplifier.

Another technique uses fast startup circuits. By reducing the startup time of the sample-and-hold reference systems, the on time of the band-gap core and scaling amplifier circuits are reduced significantly. This improves the on-to-off time ratio, thus bringing the average current down in the nanoampere range while maintaining noise and accuracy levels.

To improve the line transient response, feed-forward techniques are applied to the voltage regulation loop in an energy-efficient way. Using transient detection circuits to adjust bias currents or enable circuitry further reduces both voltage dips at the output and settling times.

**Figure 11** illustrates the application of these techniques in the TPS63900. The line transient is barely visible on the output voltage and far below the switching ripple, whereas other devices show 100-mV changes.

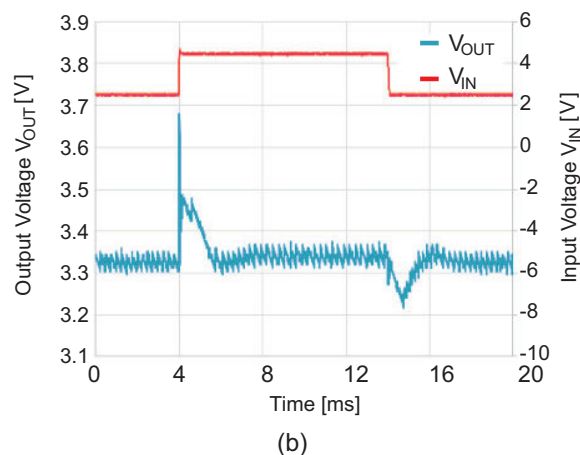
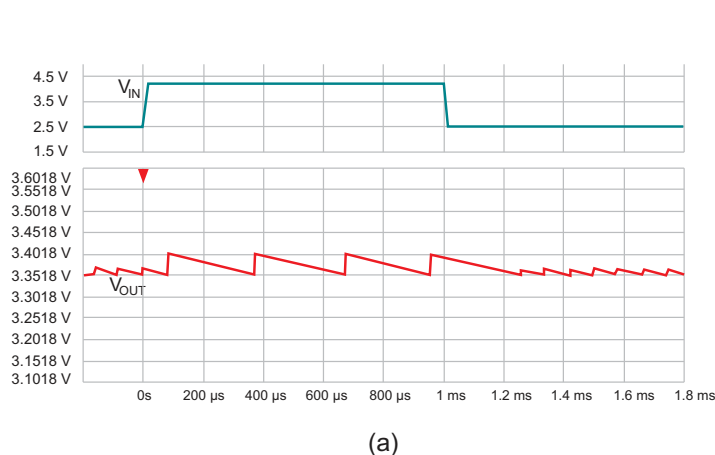


**Figure 11.** Line transient response with  $V_{IN} = 2.5\text{ V}$  to  $4.2\text{ V}$ ,  $V_{OUT} = 3.3\text{ V}$ ,  $I_{OUT} = 1\text{ mA}$ : TPS63900 (a); competing device (b).

### Addressing switching-noise issues

When designing a high-precision data application, one priority is to control the switching noise of the DC/DC converter, especially in power-save modes with transient bursts that generate a high output voltage ripple. One way to reduce ripple is to minimize the energy package sent to the output in a switching cycle. But what if that's not enough?

The **TPS62840** buck converter, which has an  $I_Q$  of 60 nA, has a STOP pin that immediately stops the regulator switching after the current switching cycle, opening a window of complete switching silence (see **Figure 12**).

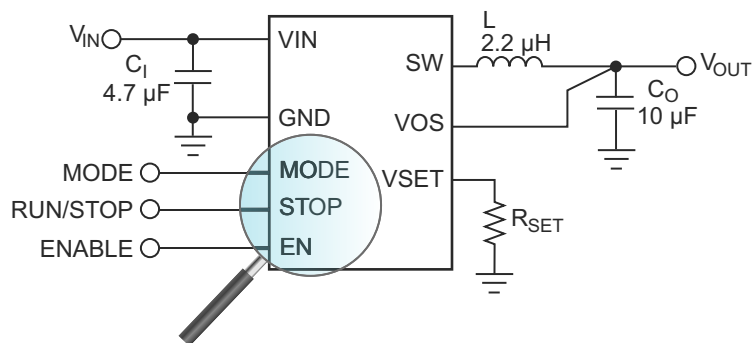


**Figure 12.** Zero switching noise on the TPS62840 from the STOP pin feature.

### Addressing other noise issues

Beyond switching noise, continuous self-noise, with thermal and flicker noise components in the range of 0.1 Hz to 100 kHz, are of concern at lower  $I_Q$  biasing. Because the reference is usually the largest noise

contributor, choosing integrated versions of sample-and-hold techniques to create both voltage and current references offer a compelling trade-off between area, noise,  $I_Q$  and robust performance (no drift) over the life of the device. The drawback of such sample-and-hold circuits are the small ripple errors created.

**Figure 13** illustrates a design using TI's precision digital-to-analog converter (DAC) and operational amplifier families that attempts to optimize sample-and-hold operation so that any glitch created is well within the noise floor of the regulator in question. Some of these techniques are employed to remove the glitch and unwanted tones in **TPS7A02** LDO design. As shown in **Figure 14**, the TPS7A02 device's sample-and-hold noise-shaping reduces integrated noise >40% in the 10- to 100-Hz frequency band.

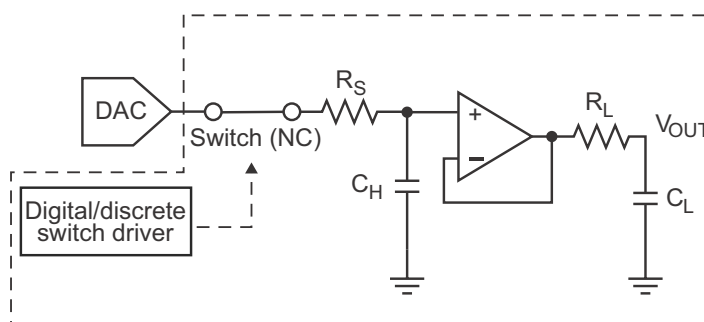


**Figure 13.** Discrete sample-and-hold DAC system.



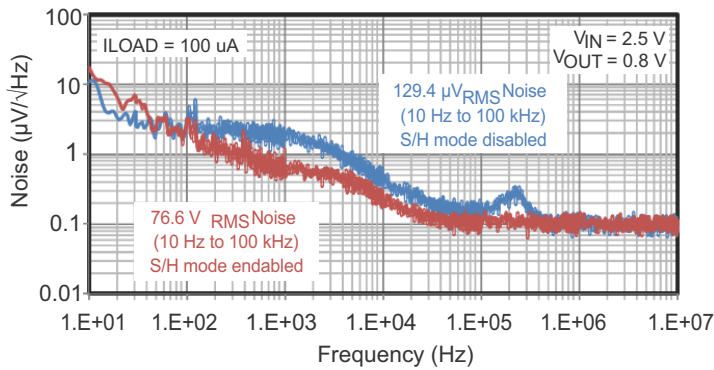


**Figure 14.** Noise spectrum with and without a sample-and-hold reference on the TPS7A02. (Source: TI internal silicon measurements on the TPS7A02).

### Addressing die size and solution area issues

One of the largest-area blocks in nanopower regulators is the current reference, which is responsible for creating 1- to 10-nA bias legs. The current bias generation area within the current reference block is dominated by resistor components. Applying smaller voltage biases across small-value resistors will reduce resistor values. One technique generates  $\Delta V_{gs}/R$  or  $\Delta V_{be}/R$  circuits when forming a reference bias current.

**Figure 15** shows a clever implementation of an almost zero-temperature coefficient bias current, creating positive and negative coefficient temperature bias currents with a small voltage bias across resistors  $R_1$  and  $R_{bias}$ .

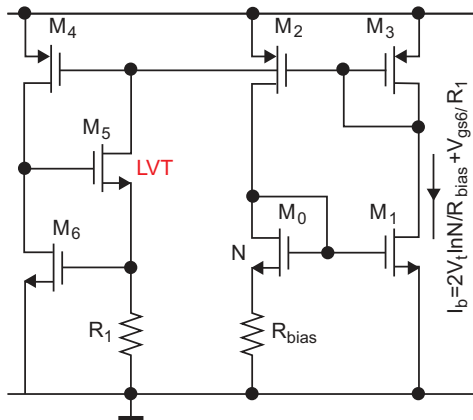


**Figure 15.** Circuit diagram of low-area 1-nA current reference.

These techniques enable a lower passive area, and effectively a smaller die area. The  $I_Q$ -multiplied-by-smallest-package-area FOM is the best way to compare

the area efficiency of such techniques. The TPS7A02 device was released in a 1-mm-by-1-mm dual-flat-no-leads (DQN) package in 2019, while its wafer chip-scale package (WCSP) counterpart released in 2021. This LDO boasts one of the industry's lowest- $I_Q$ -package-area-efficiency FOMs at  $<10 \text{ nA}\cdot\text{mm}^2$ . **Figure 16** demonstrates a side-by-side comparison of the typical 0402 capacitor vs the DQN and WCSP package offered for TPS7A02.

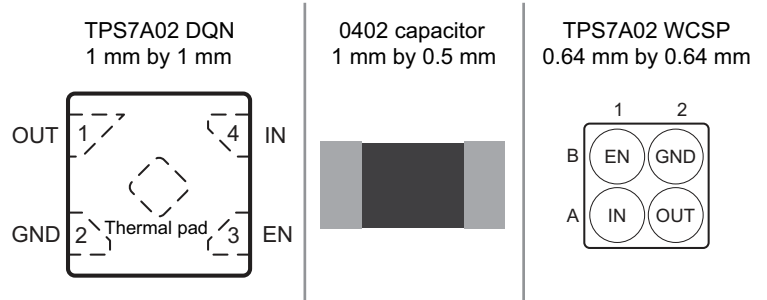


**Figure 16.** Side-by-side size comparison of TPS7A02 in a DQN package, 0402 capacitor and WCSP package.

When applying similar area-reduction techniques to supply voltage supervisors, the primary challenge will be how to sense voltages  $>10 \text{ V}$  and still achieve  $I_Q$  levels  $<0.5 \mu\text{A}$ . Capacitive sensing of the monitored voltage, combined with sample-and-hold techniques, can reduce the die area and improve the response time. The **TPS3840** nanopower high-input voltage supervisor has an  $I_Q <350 \text{ nA}$ , achieving a reset propagation delay as low as  $15 \mu\text{s}$  while directly monitoring 10-V rails.

One of the most compelling ways to save board area is to integrate more functions onto a single die. This integration enables blocks like the supervisor, reference system, LDO, battery charger and DC/DC converter to share common building blocks while reducing the combined  $I_Q$ . **Figure 17** demonstrates the ability of the **BQ25125**, a battery charge management IC, to integrate and flexibly control multiple low- $I_Q$  functions with  $I_2C$ , which gives it a key advantage to bring an entire power-management system to wearable, metering and automotive sensor IoT applications.

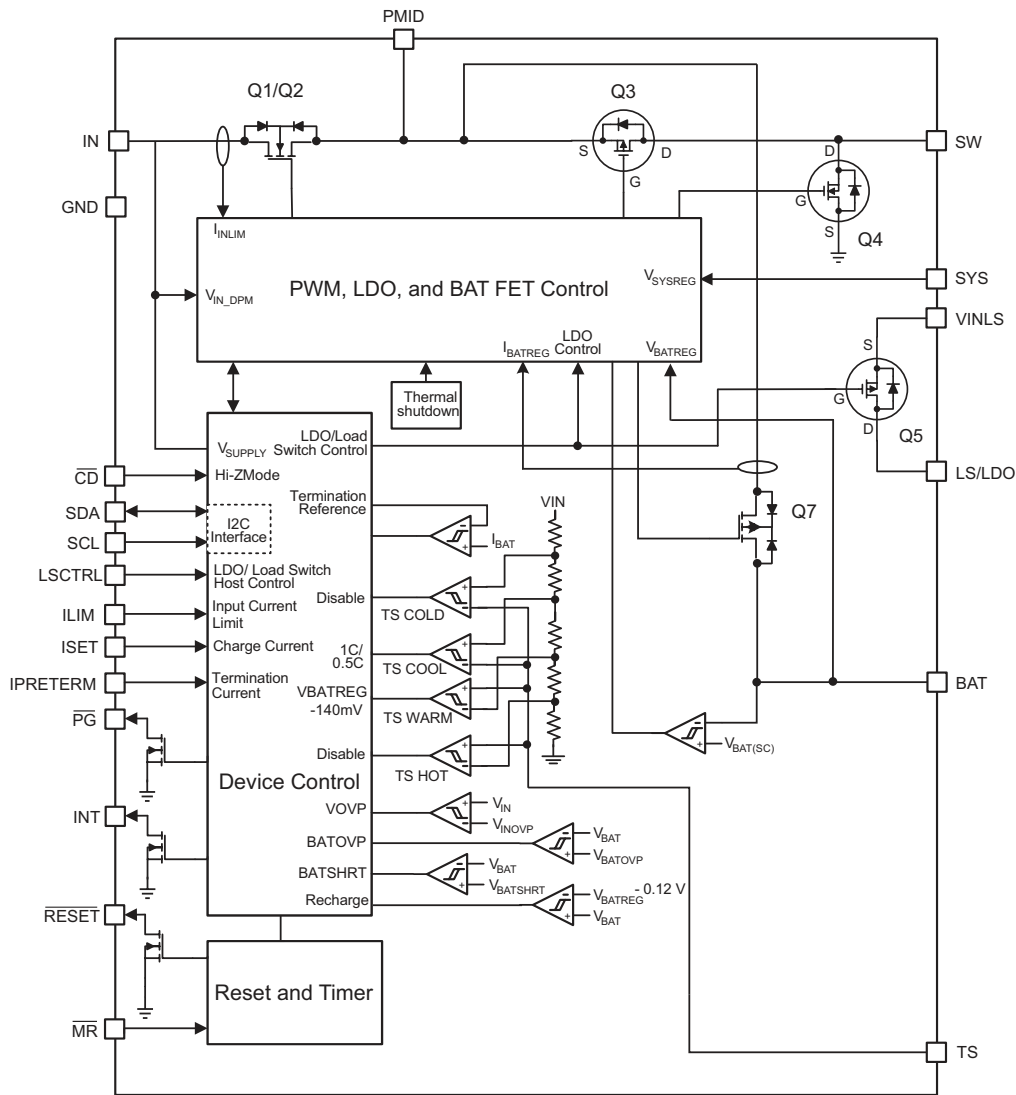


**Figure 17.** System-level diagram of a nanoampere charger system.

### Addressing leakage and subthreshold operation issues

TI power process technologies feature optimized low-power design components. High-density resistors and capacitors combined with novel circuit techniques enable a reduction in both  $I_Q$  and die area. Power FETs and digital logic provide low-leakage transistors while simultaneously being optimized for speed; thus,  $I_{SHDN}$  and area are not exclusively compromised. Additionally, accurate modeling of subthreshold operation at lower  $V_{GS}-V_T$  levels – as shown in **Figure 18** – enables reliable operation down to the picoampere/micrometer biasing level.

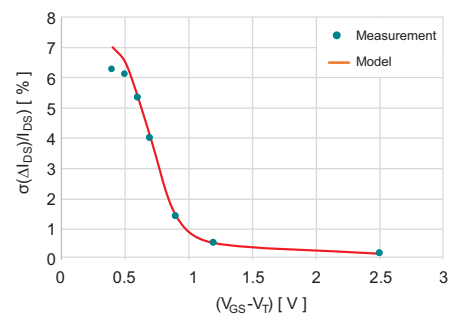


**Figure 18.** Sigma IDS percentage mismatch vs.  $V_{GS}-V_T$ .

## Electrical Characteristics

Specified at  $T_J = -40^{\circ}\text{C}$  to  $+125^{\circ}\text{C}$ ,  $V_{IN} = V_{OUT(nom)} + 0.5\text{ V}$  or  $2.0\text{ V}$  (whichever is greater),  $I_{OUT} = 1\text{ mA}$ ,  $V_{EN} = V_{IN}$ , and  $C_{IN} = C_{OUT} = 1\text{ }\mu\text{F}$  (unless otherwise noted). Typical values are at  $T_J = 25^{\circ}\text{C}$ .

Parameter		Test Conditions	Min	Typ	Max	Unit
	Nominal accuracy	$T_J = 25^{\circ}\text{C}$ , $V_{OUT} \geq 1.5\text{ V}$ , $1\text{ }\mu\text{A}(1) \leq I_{OUT} \leq 1\text{ mA}$	-1		1	%
		$T_J = 25^{\circ}\text{C}$ ; $V_{OUT} < 1.5\text{ V}$	-15		15	mV
	Accuracy over temperature	$V_{OUT} \geq 1.5\text{ V}$	-1.5		1.5	%
		$V_{OUT} \geq 1.5\text{ V}$	-20		20	mV
$(\Delta V_{IN})$	Line regulation	$V_{OUT(nom)} + 0.5\text{ V} \leq V_{IN} \leq 6.0\text{ V}^1$			5	mV
$\Delta V_{OUT}$ ( $\Delta I_{OUT}$ )	Line regulation <sup>2</sup>	$1\text{ mA} \leq I_{OUT} \leq 200\text{ mA}$ , $V_{IN} = V_{OUT(nom)} + 0.5\text{ V}^{(2)}$	$T_J = -40^{\circ}\text{C}$ to $+85^{\circ}\text{C}$	20	38	mV
			$T_J = -40^{\circ}\text{C}$ to $+125^{\circ}\text{C}$		50	
$I_{GND}$	Ground current	$I_{OUT} = 0\text{ mA}$	$T_J = 25^{\circ}\text{C}$	25	46	nA
			$T_J = -40^{\circ}\text{C}$ to $+85^{\circ}\text{C}$		60	
$I_{GND}/I_{OUT}$	Ground current vs load current	$5\text{ }\mu\text{A} \leq I_{OUT} < 1\text{ mA}$	$T_J = 25^{\circ}\text{C}$	1		%
		$1\text{ mA} \leq I_{OUT} < 100\text{ mA}$		0.25		
		$I_{OUT} \geq 100\text{ mA}$		0.15		
$I_{GND(DO)}$	Ground current in dropout <sup>3</sup>	$I_{OUT} = 0\text{ mA}$ , $V_{IN} = 95\% \times V_{OUT(nom)}$	$T_J = 25^{\circ}\text{C}$	25		nA
$I_{SHDN}$	Shutdown current	$V_{EN} = 0\text{ V}$ , $1.5\text{ V} \leq V_{IN} \leq 5.0\text{ V}$ , $T_J = 25^{\circ}\text{C}$	$T_J = 25^{\circ}\text{C}$	3	10	nA

**Table 1.** Variation of  $I_{GND}$  and  $I_{SHDN}$  in the TPS7A02 data sheet.

Variations in  $I_{Q-GND}$ ,  $I_{SHDN}$  and  $V_{OUT}$  accuracy are all good indicators of the manufacturability of a process technology's components. **Table 1**, from the TPS7A02 data sheet, lists that  $I_{GND}$  at no load varies 25 nA to 60 nA over a  $-40^{\circ}\text{C}$  to  $85^{\circ}\text{C}$  temperature range. This variation across temperature is representative of current mirror mismatch and  $I_{BIAS}$  generation control. The  $I_{SHDN}$ , which varies from 3 nA to 10 nA at room temperature, is a good indicator of power FET and digital logic leakage control.  $V_{OUT}$  accuracy is  $<1.5\%$  over temperature, which is a good indicator of subthreshold mismatch control.

### Avoiding potential system pitfalls in a low- $I_Q$ designs

The leakage of external capacitors is a concern. Both the input and output capacitors of any regulator adds to  $I_Q$ . An excellent way to evaluate the leakage of external capacitors is described in **Figure 19**, where the voltage droop is measured on the capacitor vs. time for different capacitor insulation resistance ( $R_p$ ) specifications. It's a

good idea to measure the leakage on the capacitors independent of what the data sheet says. Charging a capacitor to a known voltage and monitoring the droop over time is an excellent way to quantify and compare different capacitor options. The capacitor with the largest insulation resistance will show the least droop over time.

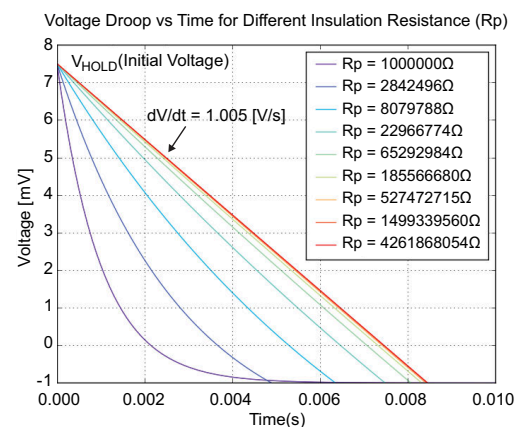


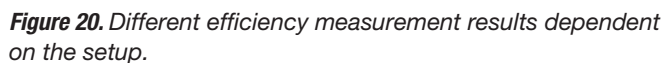
**Figure 19.** Voltage droop vs. time for different insulation resistances.

<sup>1</sup>  $V_{IN} = 2.0\text{ V}$  for  $V_{OUT} \leq 1.5\text{ V}$ .

<sup>2</sup> Load Regulation is normalized to the output voltage at  $I_{OUT} = 1\text{ mA}$ .

<sup>3</sup> Specified by design

It is possible to avoid measurement errors with the correct measurement methods and the correct placement of volt and current meters. **Figure 20** shows the impact on efficiency with different test setups, which become quite significant already lower than a 0.1 mA load. For tips on the best options to avoid setup issues for ultra-low  $I_Q$  measurements, see the Analog Design Journal article, “**Accurately measuring efficiency of ultra-low- $I_Q$  devices.**”



Flexibility is key in a low-power application design. One such example is changing the output voltage value. The traditional way is to use an adjustable external feedback divider, but this will cause not just higher inaccuracy but also higher  $I_Q$ . Modern nanoampere power converters use R2D interfaces (**Figure 21**), which enable the digitized setting of output voltages without consuming extra current, since the function will shut down after booting the device.



In harsh automotive environments, external resistors limit  $I_Q$  at the system level. Given requirements to prevent leakage, resistors are usually limited to lower than 100 k $\Omega$ . But you don't have to abandon your low- $I_Q$  and  $I_{SHDN}$  ambitions. An external feedback divider monitoring 12 V will result in an  $I_Q$  in the >100  $\mu$ A range. You could use an internal feedback divider with higher resistance to reduce the divider current, but at the cost of losing programmability.

Similar to the LM5123-Q1, the LMR43610/20 36-V, 1-A/2-A buck converter utilizes a novel approach to minimizing  $I_Q$  by integrating the feedback network. The

LMR43610/20 runs an impedance check at startup on the VOUT/FB pin, which senses the presence of an external feedback network that engineers can employ to leverage the adjustable output voltage feature. If no external feedback resistors are detected, the device will automatically utilize the integrated feedback network that sets a fixed 3.3-V or 5-V output voltage. This minimizes leakages through the feedback network and lowers  $I_Q$ .

Many switch-mode power devices like LMR43610/20 use an internal LDO to provide power to the internal circuitry for the IC. Low-voltage applications will typically supply this internal LDO directly from the input voltage. However, this method of powering the internal LDO poses a unique challenge in designs that operate across wide input voltage as the power loss from the LDO is directly proportional to input voltage.

To address it, rather than drawing power from the input, the LMR43610/20 leverages the same voltage from the VOUT/FB pin to power the internal LDO, which then biases all internal circuitry in order to minimize the total  $I_{Q\_VIN}$ . This decreases the internal LDO current by a factor of  $V_{OUT} / (V_{IN} * \eta_1)$ . These features, paired with the methods discussed throughout this paper, enable the LMR43610/20 to have best-in-class  $I_Q$  of  $<3 \mu A$  (max.) at  $150^\circ C T_J$ , and light-load efficiency of almost 90% at 1 mA for nominal 12- $V_{IN}$ , 3.3- $V_{OUT}$ , 2.2-MHz conversions.

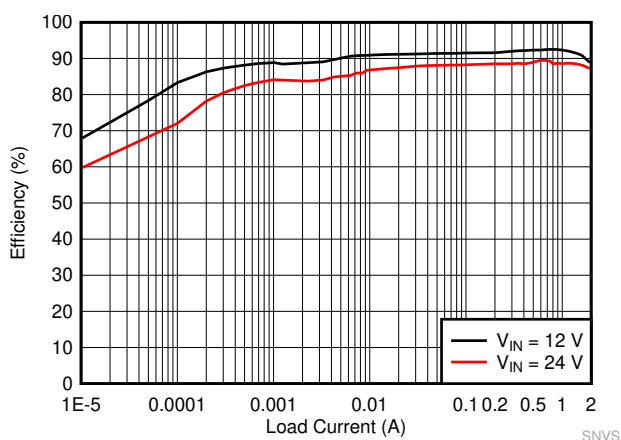


**Figure 23.** Efficiency:  $V_{OUT} = 3.3 V$  (Fixed), 2.2 MHz

## Smart on or enable features supporting low- $I_Q$ at the system level

Device-level improvements can simplify system-level designs. One such example is the smart enable feature found on the **TPS22916**, a 60-m $\Omega$ , 10-nA leakage load switch. In addition to the ultra-low leakage and  $I_Q$  performance, this device also offers a smart way to turn the switch on. Usually there is an internal pulldown at the ON pin to ensure that the power switch does not turn on accidentally in case the microcontroller controlling the switch goes into a high impedance state. These pullup and pulldown resistors unfortunately negatively impact system-level  $I_Q$ .

As shown in **Figure 24**, the TPS22916, like many nano- $I_Q$  products, has smart on or enable circuitry that opens the pulldown path after soft start, eliminating the previous always-on  $I_Q$  and still guaranteeing a known low impedance state when the device is powered off.

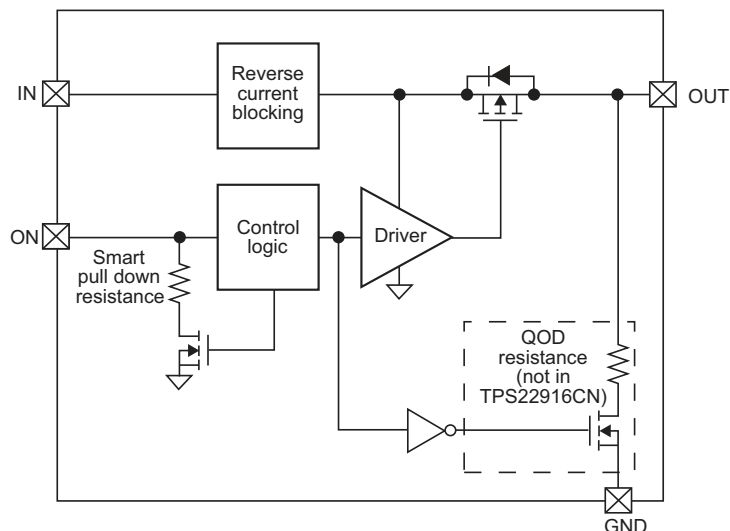


**Figure 24.** Smart-enabled circuit guaranteeing low impedance for the ON pin when device is turned off.

## Conclusion

The trend toward lower currents is clear. The need to achieve high efficiency at no- or light-load conditions requires power solutions to tightly regulate the output while maintaining ultra-low supply current. With TI's portfolio of ultra-low  $I_Q$  technologies and products, you can maximize your battery run time and enable low power consumption in your next design.

The key benefits of TI technologies for low  $I_Q$  include:

- Low, always-on power — long battery run times, enabled by ultra-low leakage process technologies and novel control topologies.
- Fast response times — fast wake-up comparators and zero- $I_Q$  feedback control enable fast dynamic responses without compromising low power consumption.
- Reduced form factors — area reduction techniques for resistors and capacitors facilitate integration into space-constrained applications while not affecting quiescent power

See [ti.com/lowiq](https://ti.com/lowiq) to learn more about how TI can help you extend battery and shelf life without compromising system performance.

## Key product categories for low $I_Q$ :

- [Battery charger ICs](#)
- [Buck-boost & inverting regulators](#)
- [Linear regulators \(LDO\)](#)
- [Power switches](#)
- [Series voltage references](#)
- [Shunt voltage references](#)
- [Step-down \(buck\) regulators](#)
- [Step-up \(boost\) regulators](#)
- [Supervisors & reset ICs](#)

**Important Notice:** The products and services of Texas Instruments Incorporated and its subsidiaries described herein are sold subject to TI's standard terms and conditions of sale. Customers are advised to obtain the most current and complete information about TI products and services before placing orders. TI assumes no liability for applications assistance, customer's applications or product designs, software performance, or infringement of patents. The publication of information regarding any other company's products or services does not constitute TI's approval, warranty or endorsement thereof.

All trademarks are the property of their respective owners.



## IMPORTANT NOTICE AND DISCLAIMER

TI PROVIDES TECHNICAL AND RELIABILITY DATA (INCLUDING DATASHEETS), DESIGN RESOURCES (INCLUDING REFERENCE DESIGNS), APPLICATION OR OTHER DESIGN ADVICE, WEB TOOLS, SAFETY INFORMATION, AND OTHER RESOURCES "AS IS" AND WITH ALL FAULTS, AND DISCLAIMS ALL WARRANTIES, EXPRESS AND IMPLIED, INCLUDING WITHOUT LIMITATION ANY IMPLIED WARRANTIES OF MERCHANTABILITY, FITNESS FOR A PARTICULAR PURPOSE OR NON-INFRINGEMENT OF THIRD PARTY INTELLECTUAL PROPERTY RIGHTS.

These resources are intended for skilled developers designing with TI products. You are solely responsible for (1) selecting the appropriate TI products for your application, (2) designing, validating and testing your application, and (3) ensuring your application meets applicable standards, and any other safety, security, or other requirements. These resources are subject to change without notice. TI grants you permission to use these resources only for development of an application that uses the TI products described in the resource. Other reproduction and display of these resources is prohibited. No license is granted to any other TI intellectual property right or to any third party intellectual property right. TI disclaims responsibility for, and you will fully indemnify TI and its representatives against, any claims, damages, costs, losses, and liabilities arising out of your use of these resources.

TI's products are provided subject to TI's Terms of Sale (<https://www.ti.com/legal/termsofsale.html>) or other applicable terms available either on [ti.com](https://www.ti.com) or provided in conjunction with such TI products. TI's provision of these resources does not expand or otherwise alter TI's applicable warranties or warranty disclaimers for TI products.

Mailing Address: Texas Instruments, Post Office Box 655303, Dallas, Texas 75265  
Copyright © 2021, Texas Instruments Incorporated